Temperature Homogenisation in an Electric Arc Furnace Steelmaking Bath

G. CAFFERY[1], D. WARNICA[2], N. MOLLOY[3], M. LEE[1]

1. BHP Research - Newcastle Labs, Shortland, NSW, 2303, Australia
2. Hatch Associates, Mississauga, Ontario, LSK 2R7, Canada
3. Department of Mechanical Engineering, University of Newcastle, Callaghan, NSW, 2308, Australia

ABSTRACT

Investigations on temperature homogenisation of the molten steel bath in and electric arc furnace indicated a complex pattern of flow and heat transfer. The parallel development of physical and computational models was undertaken. The necessity to model this multiphase flow of steel arose in an arc melting furnace in which additional oxygen refining techniques are applied in a vessel whose shape had been modified: to an eccentric non-uniform ovoid, from the traditional cylindrical bowl with a spherical bottom, in order to accommodate material handling requirements. Thermal inhomogeneity was evident on occasion in an operating furnace. The flow model was to provide a basis for operational optimisation of the existing furnace and subsequently for the optimal design of any new furnace.

The current focus is on improving thermal homogeneity in the balcony of the hearth of the arc furnace at Sydney Steel Mill. A one third scale, isothermal, physical model provided valuable insights into the surface phenomena associated with high velocity impingement of the jets from a proprietary lance system. But it was the CFD model incorporating energy fluxes driving coupled flows that showed the real complexities of the system. The dominance of the convective flows, under some conditions, calls into question the use of isothermal physical models of complex high temperature metallurgical reactors as a sole means of investigating flows without consideration of convection effects in high temperature gradients with high density liquids.

Results show that the flow and temperature patterns within the steel bath are strongly dependent on the position and operating flow rate of both the oxygen lance and the bottom bubbling system.

NOMENCLATURE

d_o	Bubble diameter (m)
g	gravitational constant (m/s^2)
h	Heat Transfer Coefficient (W/m^2K)
$\dot{m}$	Mass flow rate (kg/s)
p	momentum flow rate ($kg.m/s^2$)
q	heat flux (W/m^2)
q_o	Bottom bubbling gas flow rate (m^3/s)
r	radius of bubble plume (m)
$r_{1/2}$	50% radius (m)
T	Steel Temperature (K)
T_a	Ambient Temperature (K)
T_o	Water Cooled Panel Temperature (K)
T_{ref}	Reference Temperature (K)
v	fluid velocity (m/s)
z	vertical height in bubble plume (m)

β	Coefficient of thermal expansion (1/K)
ΔH	Heat of reaction (J/kg)
δ	Porosity (-)
δ_o	Base porosity (-)
ε	surface emissivity (-)
λ_p	Fraction of momentum transferred to bath(-)
λ_q	Fraction of heat transferred to bath (-)
ρ	density (kg/m^3)

ρ_g density of gas (kg/m^3)
ρ_l density of liquid (kg/m^3)
ρ_o density of steel at T_{ref} (kg/m^3)
σ Stefan-Boltzman constant (W/m^2K^4)

1. INTRODUCTION

Physical modelling of fluid flow in the hearth commenced with ad-hoc modelling, at full scale, of the variation in impact pattern of oxygen gas jets when a change in practice from the use of twin black pipe lances to a proprietary supersonic twin nozzle lance with flexibility in angular and range positioning was to be made. Subsequently a one third scale model was built to examine flow in the bath associated with the impinging jets. This model in turn drew attention to an extreme sensitivity of mixing pattern to the initial configuration of the jet/bath geometry. With the acquisition of a new flow package at BHP the development of a CFD model commenced with the modest target of simulating the isothermal model to examine the sensitivity to the input momentum conditions. Systematically other conditions were then added to approach a better description of the process. The conversion to a non-isothermal model produced interesting results which would be very difficult or impossible to reproduce in an isothermal transparent physical model.

The CFD model at its present stage of development is still only a single phase liquid bath. It does not attempt to simulate the complex surface wave and dispersion phenomena evident in the prototype and the isothermal scale model but it is still possible to provide insights into fluid flow and heat transfer phenomena in the hearth. Such insights may assist in the assessment and optimisation of heat transfer to eliminate furnace cold and hot spots, thus enhancing bath homogeneity. The modelling work can be extended to assess the relative merits of different hearth geometries and AC versus DC furnaces.

Results indicate the lance position has a large influence on the temperature field in the furnace. This suggests every effort should be made to standardise the positioning of the lance. Results also show an optimum bottom bubbling flowrate exists where the size of individual recirculation cells is maximised while the interaction between cells is insignificant.

2. LITERATURE REVIEW

Szekely, McKelliget and Choudhary (1983) developed a mathematical model to describe heat transfer and fluid flow in both the plasma region and the molten bath of a D.C. arc furnace. This work was one of the first attempts at modelling an EAF. It describes all major fluid dynamics phenomena that were present in the EAF steelmaking process of the mid eighties. However, the model was an axisymmetric two dimensional flow. A three dimensional model of a furnace is now feasible. EAF practices have also changed with the use of Eccentric Bottom Tapping (EBT) furnaces giving a non cylindrical shape, and oxygen injection as both a means of bath refining and a supplementary energy source.

Wunsche and Simcoe (1984) described the thermomechanical effects responsible for the shape and location of the submerged arcs used in EAF operations. They presented an equation describing the resultant axial component of the contracting force acting on the arc column and hence the pressure exerted on the molten steel surface by the impinging arcs.

More recent computational work treats heat transfer and fluid flow in the plasma region of the furnace. Qian, Farouk and Matharasan (1995) developed a model similar to that of Szekely et al. with only the plasma region solved for. The aim of their work was to determine the relative importance of various modes of heat transfer from the electric arc. Using their model they determined the most efficient operating conditions for heat transfer to the metal bath. An outcome of their work showed the heat transfer efficiency from the plasma to the steel was in the order of 30%.

Gardin et al. (1992) have simulated flow patterns in the plasma region of the EAF. The work reported to date has been preliminary in nature.

Zhang and Fruehan (1993) constructed a ¼ scale isothermal water model to study gas stirring in an electric arc furnace. They looked at the effects of bottom bubbling gas flow rate

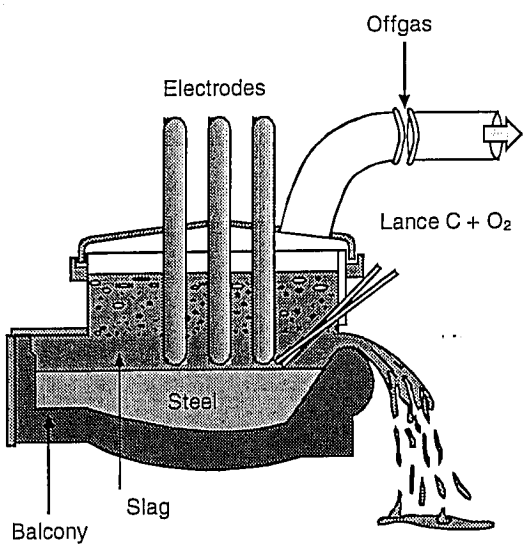

Figure 1: Diagram of an EAF

TASCflow™, a commercial finite volume/finite element based computational fluid dynamics (CFD) package, was used to develop the model. The model is a geometrically accurate representation of the Sydney Steel Mill furnace and includes such physical phenomena as;

1. heating effects of the three arcs,
2. the exothermic heat of reaction of oxygen with carbon,
3. momentum transfer from the oxygen jet to the liquid bath,
4. buoyancy effects to account for natural convection,
5. conjugate heat transfer between the liquid steel and refractory, and,
6. effects of bottom bubbling with an inert gas.

3.1 Boundary Conditions

3.1.1 Flow Field Boundary Conditions

A moving wall boundary condition was used to model the momentum transfer from the gas to the bath. Its velocity is capable of being changed to account for different gas flow rates and lance position. The momentum transferred to the bath can be represented by

$$p = \lambda_p \dot{m} v \qquad (1)$$

Where λ_p ranges from 0 to 1 and represents the fraction of momentum transferred from the gas jets to the liquid. Presently the value for λ_p is 0.03. However as both Peaslee[7] and Whitney[12] have demonstrated the cavity mode and hence amount of gas jet momentum transfer to the liquid bath is a function of oxygen lance flow rate, inclined angle and height above the bath. To more closely represent the physical prototype further work must be done to characterise the gas jet momentum transfer as a function of these variables.

A slip wall boundary condition is applied to the steel top surface. While the top surface will experience a drag force due to the slag layer the slip boundary condition is a suitable initial approximation. The validity of this assumption will be examined once a better representation of the furnace has been developed.

The remaining flow field boundary condition is the non slip boundary condition specified at the refractory/steel bath interface. Figure 2 show the flow field boundary conditions used by the model.

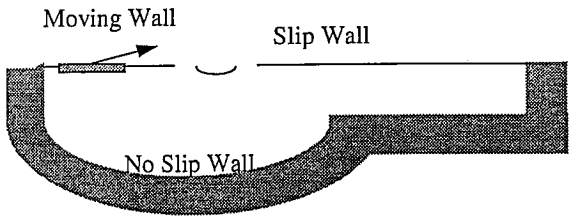

Figure 2: Flow Field Boundary Conditions

3.1.2 Heat Transfer Boundary Conditions

The exothermic heat of reaction of oxygen with the bath is accounted for by specifying a rate of heat flow at the oxygen impingement point, calculated from the equation;

$$q = \lambda_q \Delta H \dot{m} \qquad (2)$$

Where ΔH is the heat of reaction of carbon with oxygen to form CO, $\dot{m}$ is the mass flow rate of oxygen and λ_q is an empirical constant to account for the fraction of heat transferred to the steel bath. The value of λ_q was calculated to be 0.55 from a heat and mass balance at Sydney steel mill using an arc heat transfer efficiency of 30%. This is a simplification

and configuration on mixing time and two phase mass and heat transfer. They found mixing time was not a strong function of bubbler configuration and that mixing time reduced with increased stirring energy. They did not attempt to account for effects of thermal gradients on the flow field within an EAF.

Tanski (1993) developed a numerical model to predict the effects of gas stirring on bath homogeneity. The model was based on the work conducted by Zhang and Fruehan. The model assumes;

1. an axisymetric geometry,
2. isothermal flow,
3. a fixed bath surface,
4. a single point injection of gas, and,
5. bubble fluid interaction are described using a lagrangian formulation.

Results showed that as the gas flow rate increased there was an intensification of the bubble plume recirculation region.

Peaslee (1993) constructed a one half scale, two dimensional slice, isothermal water model to investigate the effects of inclined gas jetting on a liquid surface with respect to cavity formation, waves and drop formation. Jet momentum, angle of inclination and lance height above the bath were found to control the depth of gas penetration. For certain combinations of jet momentum and lance angle and position standing waves were observed. Small liquid drops were also observed to exit from the gas penetration cavity.

Following from Peaslee's work Peaslee and Robertson (1994) developed a numerical model to predict flow patterns and droplet trajectories in the cavity. Although the cavity interface is a free surface, their model treated it as a fixed wall boundary condition. This is a valid first approximation for the problem. The model predicted large drops (100μm) would strike the cavity wall and be re-entrained into the melt. Only small particles (1μm) have sufficiently low inertia to follow the flow field and escape the cavity.

Banerjee and Irons (1992) constructed a 1/10 scale model of a submerged arc electric furnace to study bottom build up and gas stirring in a nickel smelting furnace. Using a 52wt% calcium chloride solution, electric resistance heaters to represent the submerged arcs and bottom cooling from a water jacket they were able to simulate the thermal stratification that occurs in the furnace. Although not able to obtain exact similitude they found a cold stagnant layer formed at the bottom of the furnace Gas stirring reduce the thermal stratification with higher flow rates producing a more homogeneous bath. The stability of the thermal stratification increased as the heat input to the top surface increased causing a corresponding increase in thermal mixing times. They concluded that thermal effects have a significant influence on the flow field within the furnace and hence mixing time measurements with isothermal models cannot be applied to top heating vessels. This can be more generally stated that isothermal mixing times cannot be applied to processes were thermal gradients are expected.

With the exception of Banerjee and Irons all the physical models ignore the effect of thermal gradients on the flow field with in an EAF. Due to the high density of molten steel large buoyancy forces can form from small temperature gradients in the bath, influencing the flow pattern within an EAF. To accurately predict the flow pattern within the furnace and hence the level of bath homogeneity the thermal effects must be considered. The easiest method to examine thermal effects is to develop a CFD model of the process.

3. MODEL DEVELOPMENT

In the present study, the steel phase was modelled as a single phase bath flow with various input fluxes of momentum and energy. The model assumes steady state operating conditions which is equivalent to flat bath operation on the plant prototype. The model cannot account for the melt down stage of the operation nor can it predict the effect of unmelted scrap on the flow field.

Figure 1 is a schematic diagram of an EAF and shows the location of the balcony, electrodes, off gas system and oxygen lance. All of these influence the steel bath flow and temperature fields and need to be included in the model.

with the energy transfer to the steel bath being a function of;

1. the fraction of carbon reacting in the steel versus the fraction that reacts in the slag, and,
2. the heat transfer characteristics of the slag and steel phases.

To give a better representation of the heating effects will require quantification of these effects.

A radiating boundary condition is specified for the top surface which is assumed to radiate as a black body to the furnace walls at temperature T_o i.e.

$$q = \varepsilon\sigma\left(T^4 - T_o^4\right) \qquad (3)$$

This is a reasonable first approximation pending further development to include the slag phase.

For the external surface of the shell a typical heat transfer coefficient and ambient temperature are specified.

$$q = h(T-T_a) \qquad (4)$$

Figure 3 show the temperature field boundary conditions used by the model.

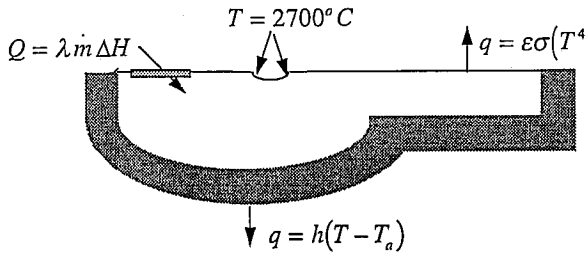

Figure 3: Temperature Field Boundary Conditions

3.2 Physical Models

3.2.1 Natural Convection

Temperature gradients exist in the bath giving rise to density differences and hence buoyancy forces creating thermally driven flows. The Boussinesq approximation is used to account for this effect. The approximation assumes the flow is incompressible and that the variation in bath density with temperature is linear and of the form,

$$\rho = \rho_o\left(1 + \beta(T - T_{ref})\right) \qquad (5a)$$

This force term is included in the momentum equation,

$$S = \rho_o g \beta (T - T_{ref}) \qquad (5b)$$

3.2.2 Bottom bubbling

Bottom bubbling aids in bath mixing mainly due to its effect on bath density resulting in a buoyancy driven recirculation. Many empirical models exist to predict the density field within a rising bubble plume. The model chosen for this purpose is that proposed by Castillejos, Salcudean and Brimacombe (1989) in which the density is defined as follows,

$$a_n = \left[\frac{g d_o^5}{q_o^2}\right]^{0.26}\left[\frac{\rho_l}{\rho_g}\right]^{0.13}\left[\frac{z}{d_o}\right]^{0.94} \qquad (6a)$$

$$r_{1/2} = 0.275\left[\frac{g}{q_o^2}\right]^{-0.2}\left[\frac{g d_o^5}{q_o^2}\right]^{0.15}\left[\frac{\rho_l}{\rho_g}\right]^{0.11}\left[\frac{z}{d_o}\right]^{0.51} \qquad (6b)$$

$$\delta_o = \min\left[\frac{0.815}{a_n^{0.1}}, \frac{1.069}{a_n}\right] \qquad (6c)$$

$$\delta = \delta_o \exp\left[-0.693\left(\frac{r}{r_{1/2}}\right)^{2.4}\right] \qquad (6d)$$

$$\rho = \delta\rho_g + (1-\delta)\rho_l \qquad (6e)$$

With the density defined by the above relationship the source term that is then added to the vertical component of momentum is simply

$$S = (\rho - \rho_o)g \qquad (6f)$$

3.3 Future Developments

Several physical effects should be included to improve the models representation of the prototype.

3.3.1 Radiative Heat Transfer Boundary Condition

The current top surface boundary condition is the simplest form of a radiative boundary condition. The melt surface is assumed to be a black body radiating to the water cooled panels of the upper shell. Absorption and reflection in

the slag phase is not taken into account neither are the heat transfer mechanisms in the hood of the furnace. Because of the strong coupling between heat transfer in the hood and the metal bath a heat transfer model of the hood should be developed to obtain an appropriate conjugate boundary condition for the bath surface.

Such a model would require experimental data for;

1. the heat transfer characteristics of the foaming slag,
2. the combustion kinetics of the oxygen/coke mixture entering the furnace, and,
3. the post combustion (burning of off gas in the head space of the furnace) kinetics of the off gases.

3.3.2 Magnetohydrodynamics

Passage of an electric current through a molten metal bath produces an electromagnetic field enhancing bath motion. For an AC furnace the induced field restricted to a localised region surrounding the arcs. In a DC furnace the electromagnetic field effects the entire bath inducing significant motion.

To quantify this effect the electromagnetic field must be determined and its influence on the flow field accounted for. This requires the solution of Maxwell's equations coupled with the hydrodynamic equations. This will allow a comparison to be made between the flow patterns of DC and AC furnaces.

4. BATH MIXING

Temperature inhomogeneity in the balcony of the EAF is a problem. Many factors influence this problem. However, the externally controllable operational parameters are;

1. lance position and flow rate,
2. bottom bubbling flow rate and nozzle type, and,
3. bottom bubbling configuration as a vessel design variable.

This model is ideally suited to investigating the effects of varying operating conditions on bath homogeneity within the furnace and in particular comparative studies in the balcony.

4.1 Supersonic Lance

Sydney Steel Mill uses a supersonic water cooled lance. It consists of two divergent nozzles having an included angle of 30°. The lance is placed in the slag door at the back of the furnace. Its position is controlled to be swept through a horizontal angle of 20° about the centre line. An optimum lance position may exist for bath homogeneity. A diagram showing the lance position is shown below in Fig. 4.

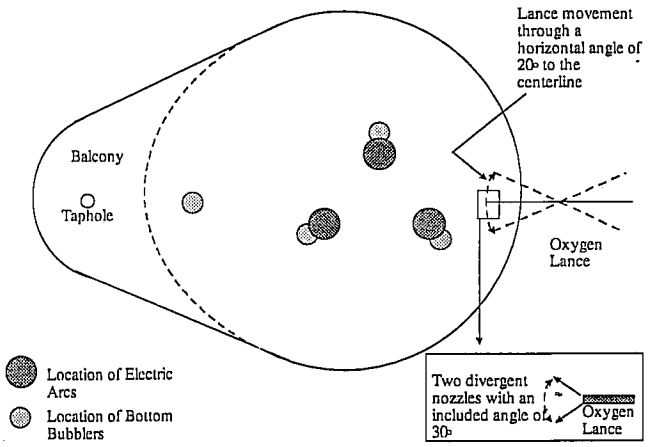

Figure 4: Layout of Oxygen Lance, Electric Arcs and Bottom Bubblers

4.2 Bottom Bubbling

The bottom bubbling system used at SSM consists of four bubblers in a pattern of three on the arc pitch circle diameter and one between the arcs and the taphole. The layout of the bottom bubbling system is shown in Figure 4. An optimum bubbler configuration and flow rate may exist for bath homogeneity.

4.3 Parametric Survey

A parametric survey was conducted to examine bath homogeneity with the aim of reducing the temperature gradient in the balcony. Parameters that were investigated include;

1. Lance direction;
2. Lance tip design;
3. Bottom bubbling configuration; and;
4. Bottom bubbling flow rate.

A list of the runs are shown below in Table 1.

Table 1: Parametric Survey Runs

Run	Lance		Bottom Bubbling	
	Position[1]	Tip Design[2]	Flow rate (Nm^3/h)	Configuration[3]
1-0	0	30	5	1
1-1	0	0	5	1
1-2	30	30	5	1
1-3	30	0	5	1
1-4	-30	30	5	1
1-5	-30	0	5	1
1-6	0	30	2.5	1
1-7	0	30	10	1
1-8	0	30	2.5	2
1-9	0	30	5	2
1-10	0	30	10	2

5. RESULTS AND DISCUSSIONS

5.1 Bath Homogeneity

Bath homogeneity is difficult to quantify. Table 2 attempts to quantify bath inhomogeneity by reporting average speeds and temperatures for the entire bath and the balcony region. With this approach subtleties in the flow and temperature fields are lost with vastly different fields giving the same values. However, it does give a general impression of the level of homogenisation.

Table 2: Representative Bath Speeds and Temperatures

Run	Avg. Bath Speed (m/s)	Avg. Bath Speed in Balcony (m/s)	Avg Bath Temp. (°C)	Avg. Bath Temp. in Balcony (°C)
1-0	0.065	0.037	1626	1601
1-1	0.070	0.035	1627	1602
1-2	0.12	0.072	1630	1623
1-3	0.14	0.10	1644	1635
1-4	0.13	0.084	1639	1629
1-5	0.15	0.12	1638	1627
1-6	0.072	0.052	1622	1617
1-7	0.076	0.058	1620	1609
1-8	0.074	0.047	1621	1616
1-9	0.065	0.036	1611	1593
1-10	0.065	0.034	1614	1594

The best method to measure bath homogeneity is a visual examination of the bath temperature profiles. As the bath becomes more homogenous the temperature gradients within the bath decrease. Figure 5 is a typical temperature field on the top surface of the bath. Its main features ares;

1. a region of hot steel in the centre of the furnace, due to the heating effects of the three arc,
2. a hot region at the oxygen impingement point, due to the combustion of carbon with oxygen, and,
3. a cold region in the balcony of the furnace.

5.2 Effects of Oxygen Lance

Comparison of Fig. 5 and 6 shows the effects of lance position on bath homogeneity. Figure 5 is the bath top surface temperature profile for run 1-0, where the lance is directed along the furnace centre line. Table 2 shows the balcony is on average 25°C colder that the rest of the furnace. Figure 6 is the temperature profile for run 1-3 where the lance is offset by 30° to the furnace centre line. While the balcony is still colder than the rest of the furnace the average bath temperature has increased and the temperature difference has reduced to 9°C.

These differences in homogeneity can be explained by comparing Fig. 7 and 8 which are the streak line plots for run 1-0 and run 1-3. A streakline is the path a massless particle would take if it were placed in the bath at a given point. The colours of the streaklines indicate the speed of the fluid at the given location.

Considering Fig. 7, the high velocity outflow from the oxygen impingement point interferes with each of the recirculation zones formed from the four bottom bubblers. As a result the flow never reaches the balcony producing a cold stagnant zone. In contrast, for Fig. 8 the outflow from the oxygen lance impingement point by-passes all of the bubblers and makes its way into the balcony of the furnace. The flow field that results is a total bath rotation, improving bath homogeneity.

5.3 Effect of Bottom Bubbling Configuration and Flow Rate

5.3.1 Effect of Gas flow rate

The effect of bottom bubbling flow rate can be seen by considering Fig. 9 - 11. These figures show the progression of the temperature profile as the bottom bubbling flow rate increases

[1] The lance position is defined as the angle the lance makes with the furnace centre line.

[2] Tip design is defined as the included angle between the lance nozzles.

[3] Configuration 1 represents the standard configuration.

Configuration 2 is the configuration of a bubbler under each arc.

from 2.5 Nm^3/hr for Fig. 9 to 5 Nm^3/hr for Fig. 10 and finally 10Nm^3/hr for Fig. 11.

These plots show that as gas flow and hence mixing energy is increased bath homogeneity decreases. This is counter intuitive but can be explained by considering the associated streakline plots.

For Fig. 12 which corresponds to a gas flow rate of 2.5 Nm^3/hr the dominatant mixing effect is caused by the oxygen lance outflow. It has sufficient momentum to bypass the bubblers, resulting in a gentle bath rotation producing a reasonably homogenous temperature profile. When the bottom bubbling gas flow rate is increased to 5 Nm^3/hr, corresponding to Fig 13, the interaction between the oxygen lance outflow and bottom bubblers become significant. The resulting flow field is more complex with a stagnant cold zone forming in the balcony.

Figure 14 shows at a bottom bubbling gas flow rate to 10 Nm^3/hr the interactions between individual bubblers dominates the flow field. The interactions between the bubblers acts to contain the steel beneath the arcs. The steel from this region is only able to exit at the three intersections of the bottom bubbling recirculation cells. At these intersections the steel is pushed out of the arc region, explaining the three hot spikes formed at the edge of the arc region.

5.3.2 Effect of Bubbler Configuration

Comparing Fig. 5 and 10 shows the importance of the fourth bubbler. In Fig. 5 the fourth bubbler is working and as a result the balcony temperature is approximately 10 °C hotter than in Fig. 10 where the fourth bubbler is absent. The present of the fourth bubbler also effects the flow field in the main furnace section which produces a more uniform temperature profile throughout the entire furnace.

5.3.3 Recommended Operation Strategy

Based on these results the following recommendations were made to improve operations at Sydney Steel Mill.

1. The oxygen lance should be directed off centre from the furnace centre line to produce a rotating bath motion.
2. The fourth bubbler should remain where it is, as it aids bath motion in the balcony.
3. For the current bottom bubbling configuration, the gas flow rate should not exceed 5 Nm^3/hr. A trial could be conducted to see if there are any benefits gained by operating at a low flow rate of 2.5 Nm^3/hr.
4. Consideration should be given to replacing the three individual bubblers beneath each arc with one bubbler in the centre of the arcs to reduce the possibility of adverse bubbler interaction.

These results are indicative, but should be treated with caution as there are several uncertainties associated with the results,

1. The arcs are modelled as a non slip wall boundary condition, which will affect the flow field in the arc region; and;
2. The model to describing bottom bubbling is an approximation but requires further development and calibration.

6. CONCLUSIONS

A model to predict flow and heat transfer effects within the EAF hearth is being developed. This model has been used to conduct a bath homogenisation study with the results of the study indicating

1. The position of the oxygen lance has a large influence on the flow field within the furnace and in particular the balcony. To maintain a homogenous bath temperature the lance should be directed at an angle to the furnace centre line.
2. Bottom bubbling configuration and flow rate influence bath mixing;
    a) The presence of the fourth bubbler in the balcony aids bath motion in this region and helps maintain a homogenous bath temperature.
    b) A critical gas flow rate exists where individual bubbler plumes begin to interact. These interactions adversely affecting bath homogenisation. For the

configurations studied here the critical flow rate is about 5 Nm^3/hr.

To reflect more closely the physical prototype several further physical effects need to be included, such as magnetohydrodynamics, multiphase flow including emulsion formation and surface effects including wave formation.

A heat transfer model of the hood should be developed to improve the top surface heat transfer condition. This would include the radiative and convective heat transfer through a foaming slag and radiative and convective heat transfer through an optically thick gas phase between the slag layer and the water cooled hood. Also included would be the effects of combustion of the carbon/oxygen mixture and the post combustion effects of the furnace off gas.

8. REFERENCES

[1] Szekely J., McKelliget J., Choudhary M., Heat transfer, Heat Transfer Fluid Flow and Bath Circulation in Electric Arc Furnaces and DC Plasma Furnace, *Ironmaking and Steelmaking*, Vol 10 No.4, 1983 pp169-179

[2] Wunshe E.R., Simcoe R., Electric Arc Furnace Steelmaking with Quasi-Submerged Arcs and Foamy Slags, *Iron and Steel Engineer*, April 1984, pp 35-42

[3] Gardin P., Soide C., Dez A., Guillaume I., Use of Physical and Numerical Simulation Methods to Characterise Gas Flow in a Trielectrode Electric Arc Furnace, *Ironmaking and Steelmaking*, Vol. 19, No. 4, 1992, pp306-309

[4] Qian F., Farouk B., Mutharasan R., Modeling of Fluid Flow and Heat Transfer in the Plasma Region of the DC Electric Arc Furnace, *Metallurgical and Materials Transactions B*, Vol. 26B, 1995, pp1057-1067

[5] Zhang X., Fruehan R.J., Modelling of Gas Stirring in An Electric Arc Furnace, *CISR Progress Report*, April 1993, pp 109-132

[6] Tanski J. Numerical Simulation of Coupled Two Phase Gas/Liquid Flow in An Electric Arc Furnace, *1993 Electric Furnace Conference Proceedings*, 1993, pp 395-399

[7] Peaslee K.D., Physical Modelling of Interaction Between a Top Blown Jet and the Slag/Metal Bath in Steelmaking, *1993 Electric Furnace Conference Proceedings*, 1993, pp 403-411

[8] Peaslee K.D., Robertson D.G.C., Fluid Dynamics of Inclined Jetting on a Slag/Metal Bath, *1994 EPD Conference*, 1994

[9] Banerjee S.K., Irons G.A., Physical Modelling of Thermal Stratification, Bottom Build-Up and Mixing in Submerged Arc Electric Smelting, *Canadian Metallurgical Quarterly*, Vol. 31 No.1, Jan. 1992, pp 31-40

[10] Advanced Scientific Computing, TASCflow Version 2.4 Users Manual, 1995

[11] Castillejos A.H., Salcudean M.E., Brimacombe J.K., Fluid Flow and Bath Temperature Destratification in Gas Stirred Ladles. *Metallurgical and Materials Transactions B*, 20B, 603-611

[12] Whitney V., Honours Year Thesis, Department of Chemical Engineering, Newcastle University, NSW Australia, 1996

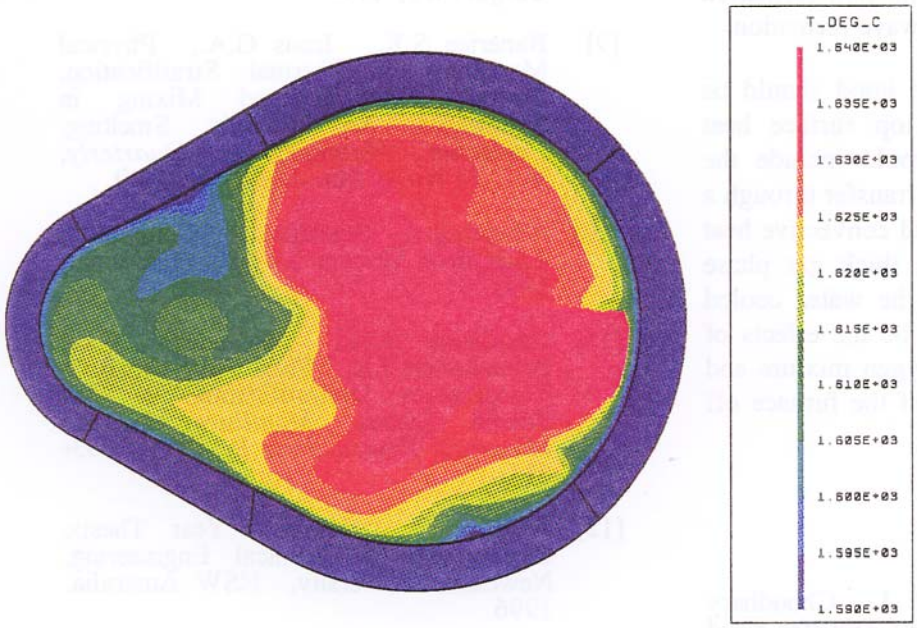

Figure 5: Temperature Plot for Run1-0

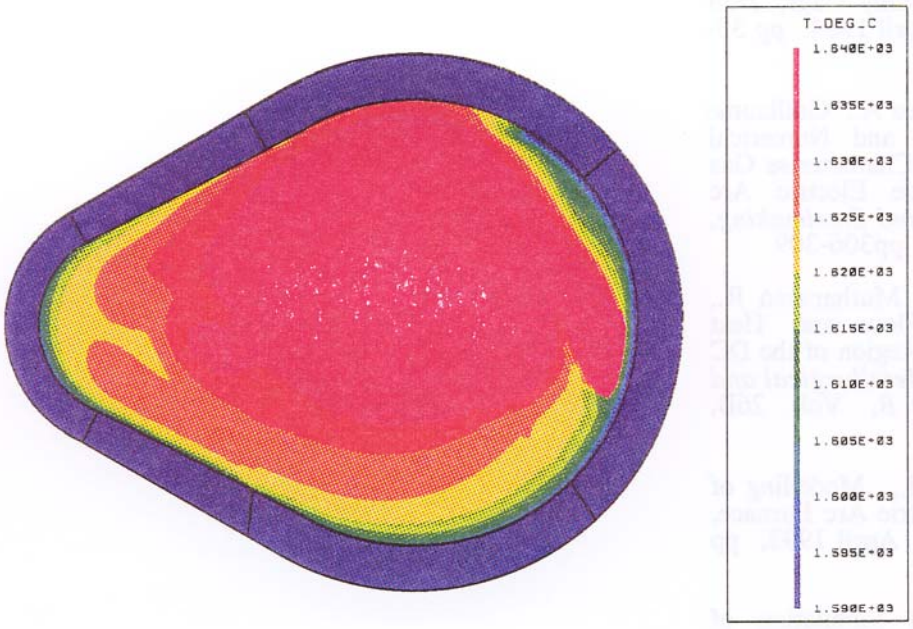

Figure 6: Temperature Plot for Run1-3

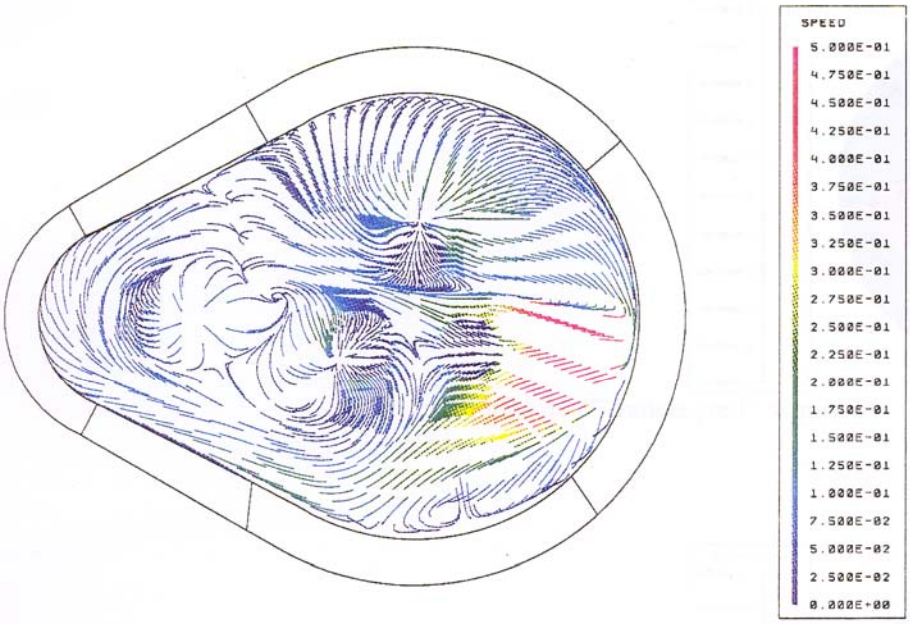

Figure 7: Streakline Plot for Run1-0

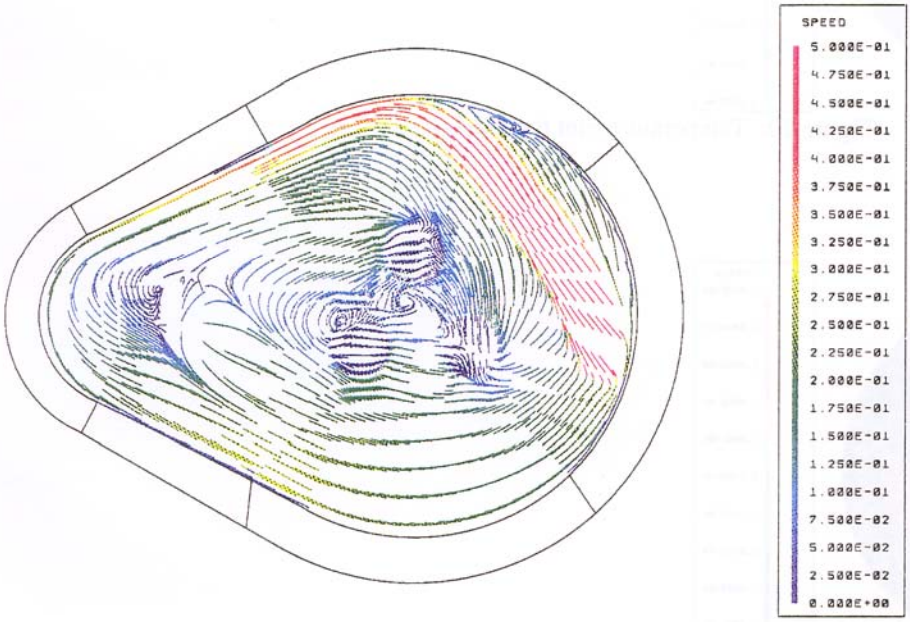

Figure 8: Streakline Plot for Run1-3

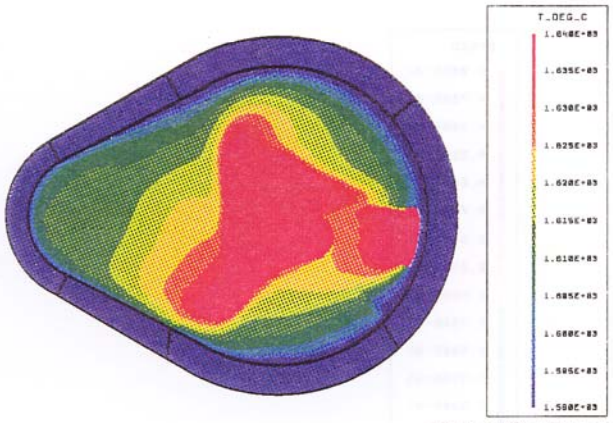

Figure 9: Temperature Plot for Run1-8

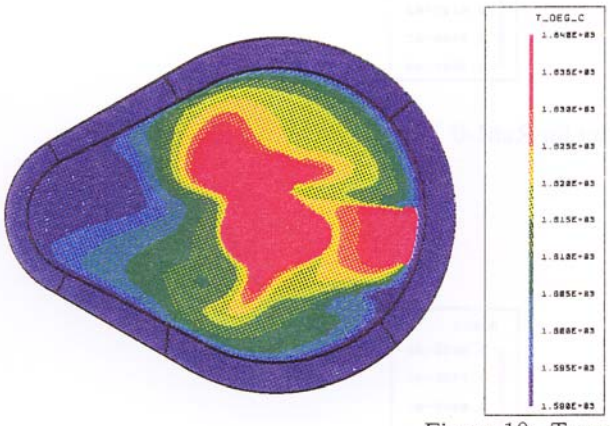

Figure 10: Temperature Plot for Run1-9

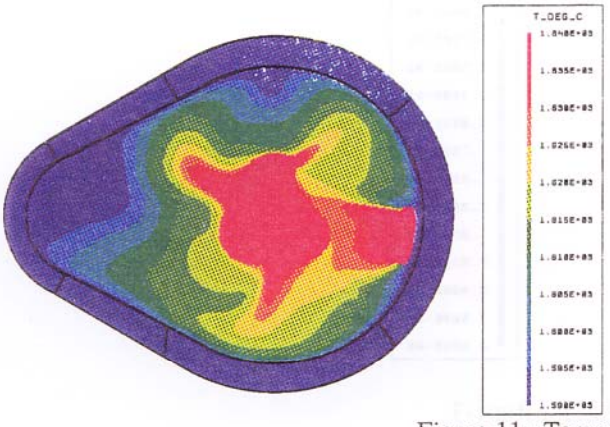

Figure 11: Temperature Plot for Run1-10

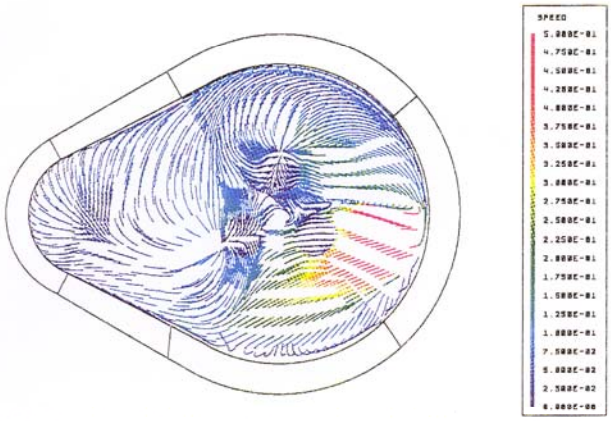

Figure 12: Streakline Plot for Run1-8

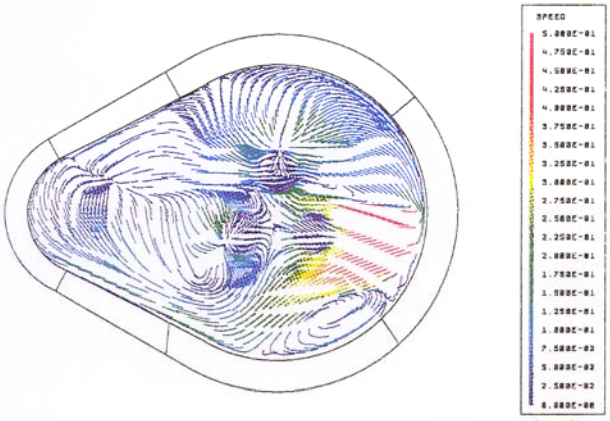

Figure 13: Streakline Plot for Run1-9

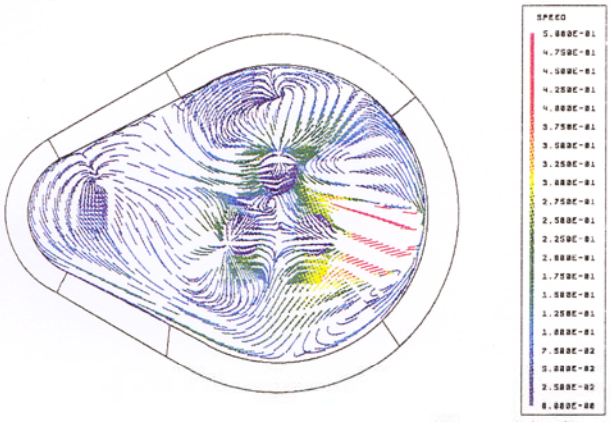

Figure 14: Streakline Plot for Run1-10